

# OPTICAL PROPERTIES OF OXIDIZED TERFENOL-D THIN FILMS OBTAINED BY PULSED LASER DEPOSITION

RUXANDA MIREANU<sup>1</sup>, VALENTIN ION<sup>2,\*</sup>, LUIZA M. STINGESCU<sup>2</sup>, OVIDIU TOMA<sup>1,\*</sup>

<sup>1</sup> University of Bucharest, Faculty of Physics, Atomiștilor Street 405, 077125 Măgurele, Romania

<sup>2</sup> National Institute of Laser, Plasma and Radiation, 077125 Măgurele, Romania

\* *Corresponding authors:* thtoma72@yahoo.com; valentin.ion@inflpr.ro

*Received July 18, 2022*

*Abstract.* This paper concentrates on the characterization of Terfenol-D thin films through spectroscopic ellipsometry measurements. All the films were obtained by pulsed laser deposition, and their topographical, morphological, chemical composition and resistivity analysis was performed through atomic force microscopy, scanning electron microscopy, and energy dispersive X-ray measurements. By ellipsometry we have computed an optical model to fit the experimental data and obtain the optical constant's dispersion. The obvious results were that the films have been oxidized, which influences the refractive index and extinction coefficient behavior to go from that of a metallic alloy to a material indicating a mixture of oxides. The results have not come as a surprise, since in the literature, most experimental trials of depositing and analyzing Terfenol-D films have encountered the same oxidation problem.

*Key words:* Terfenol-D, magnetostriction, pulsed laser deposition, oxidized thin films, spectroscopic ellipsometry.

## 1. INTRODUCTION

Thin films represent the subject of interest of many newly developed branches of physics, such as nanotechnology, biophysics, material science and solid-state physics. A deep understanding of their properties from the morphological, topographical and structural point of view is necessary in order to use them in applications. Their importance relies in the vast range of utilities, among which we mention optical and protective coatings, creation of photovoltaic cells, integration in plasmonic and biosensors devices.

The purpose of this experimental work was to obtain crystalline thin films of Terfenol-D through pulsed laser deposition. However, in the end the resulted films were rather amorphous, presenting large quantities of iron oxides on their surfaces. The oxidation issue of Terfenol is largely met in the literature, as the preferential combination of oxygen with rare earth atoms (Tb, Dy) makes the material iron-rich by forming inclusions of  $R_2O_3$  (where R stands for rare earth elements) [1].

## 2. THEORETICAL BACKGROUND

Terfenol-D is an alloy composed of two rare – earth elements (or lathanides), Terbium ( $^{65}\text{Tb}$ ) and Dysprosium ( $^{66}\text{Dy}$ ), together with iron ( $^{26}\text{Fe}$ ). The “nol” suffix comes from the Naval Ordnance Laboratory (NOL), of United States, where the material was first developed around the 1970’s. Its creation resulted from the need of reducing the magnetocrystalline anisotropy of Tb consisted in the  $\text{TbFe}_2$  alloy, which was found to have the highest magnetostriction at room temperature at that time [2]. Dysprosium in quantities of 70% was added and thus came the material  $\text{Tb}_{0.3}\text{Dy}_{0.7}\text{Fe}_2$ , the most encountered and studied form of Terfenol-D. In this paper we have obtained thin films of Terfenol-D of two different concentrations,  $\text{Tb}_{0.3}\text{Dy}_{0.7}\text{Fe}_2$  and  $\text{Tb}_{0.4}\text{Dy}_{0.6}\text{Fe}_2$  and we will refer to them by their Dysprosium percentage, as Terfenol 0.7 and Terfenol 0.6.

The study of Terfenol-D is of great interest as this alloy has unique properties, displaying the largest known magnetostriction. This feature of changing its shape and properties when subjected to a magnetic field, allows it to be used in various applications, especially in the manufacturing of sensors and actuators [3, 4]. For example, Terfenol may be used in actuation when its particles are excited with a magnetic field, causing their expansion. On the other hand, it can be used as sensors when the material is mechanically strained, action under which the particles will generate an induced voltage. This is the Villari effect which consists in the change of magnetization due to applied stress [5].

Terfenol-D is a polyhedral material with a face-centered cubic structure (Fig. 1). It also displays a polymorphic structure, meaning that it can change to different crystalline structures and still posses the same chemical composition [6].

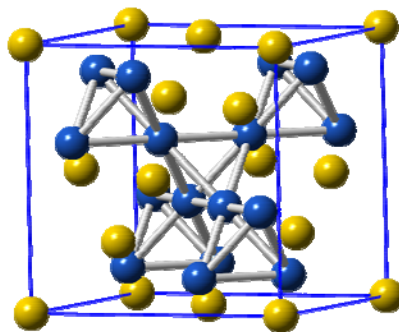


Fig. 1 – C15 lattice structure [7].

Among the physical properties we encounter a high energy density, low Young’s modulus and low fracture resistance. Indeed, the brittleness of Terfenol-D

has been known to represent a disadvantage of the material, limiting its ability to operate in tension or resist to shock loads [6, 8].

When dealing with Terfenol-D thin films one must be careful as the exposing of the films to ambient atmosphere raises the concern in oxidation issues [1]. This problem is expected since in rare earth materials the oxidation is a well-known problem which can sometimes lead to spontaneous combustion (pyrophoric materials) or material degradation. The oxidation in bulk materials can drastically reduce the magnetostriction.

The main solution in order to avoid the oxidation in thin films is to deposit a protective layer. Another method to reduce the oxidation level on Terfenol-D thin films is their dipping into acetone [9].

The utility of magnetostrictive materials gained a lot of attention in the recent years because of their potential for high volume production. There are many interesting projects which manipulate Terfenol-D in order to produce fluid injectors, active damping systems, wireless linear micro-motors, electro-hydraulic actuators, helicopter blade control systems and many more [10, 11, 12]. Terfenol-D is also used in ultrasonic cleaning, machining and welding, micropositioning and the detection of motion, force and magnetic fields [13, 14, 15].

In this paper we emphasize the optical analysis of the obtained probes which was performed by the means of spectroscopic ellipsometry, one of the most powerful techniques of optical characterization. Besides its abilities of obtaining the refractive indices, extinction coefficients and dielectric functions of certain materials, ellipsometry enhances the acquiring of film thickness, roughness, crystallinity and band gap energies. It is an indirect method which involves the study of the s- and p-components of elliptically polarized light whose magnitudes and phase difference provide the means of studying the material's optical constants [16].

For a better understanding of Terfenol-D, in the experimental procedure we have also performed Atomic Force Microscopy, Scanning Electron Microscopy, Energy Dispersive X-rays and electrical resistivity measurements, which indicated important results from topographical, morphological and chemical composition perspectives.

### 3. EXPERIMENTAL RESULTS

#### 3.1. OBTAINING METHOD (PLD)

The obtaining method of the films was pulsed laser deposition (PLD), which is a frequently encountered physical vapor deposition process (Fig. 2).

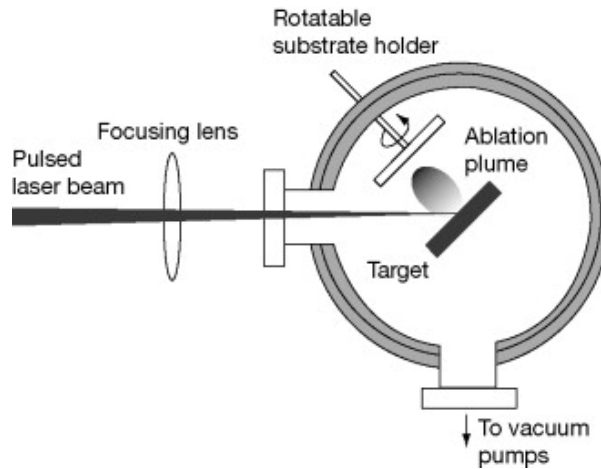


Fig. 2 – Pulsed laser deposition diagram [18].

Its functionality consists of a laser focused onto a target of the material to be deposited. For a certain energy, each laser pulse will ablate (vaporize) a small amount of the material which shall be ejected from the target and deposited as a thin film on the desired substrate. The process takes place in vacuum [17].

The used light source was the Nd:YAG solid body laser (with a 266 nm wavelength), a pulse repetition of 10 Hz. The distance between the target and substrate was maintained at all times at 4 cm. Wanting to take into consideration the role the deposition temperature plays in the influence of films properties, we had varied it, making depositions for room temperatures  $RT = 27^{\circ}\text{C}$  and temperatures of  $300^{\circ}\text{C}$ ,  $500^{\circ}\text{C}$  and  $600^{\circ}\text{C}$  using a heat rate of  $50^{\circ}\text{C}$  for the heated films and a cooling temperature of  $10^{\circ}\text{C}$  per minute. The number of pulses is 36000 per hour for all probes. It is important to mention that the deposition process took place in vacuum conditions (at pressures of  $10^{-5}$  mbar), and the laser fluence was of  $1.2 \text{ J/cm}^2$ .

The Terfenol-D films were deposited on silicon (Si) and platinum (Pt/Si) substrates.

### 3.2. CHARACTERIZATION METHODS (AFM, SEM, EDX, RESISTIVITY, SE)

The atomic force microscopy analysis revealed that all probes were covered by droplets formations (no matter the substrate nature) with heights ranging between 250 and 700 nm. The important aspect is that no probe presented crevices or cracks and that the formations were quite uniform, present on the whole surface of the films (Fig. 3).

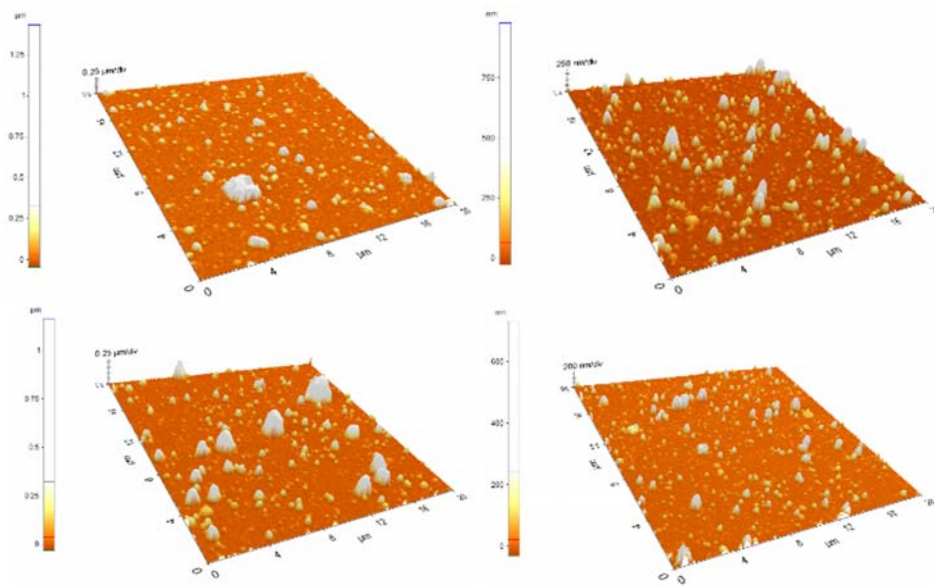


Fig. 3 – Pictures of Terfenol-D thin films deposited on different substrates.

From morphology perspective, we have performed Scanning Electron Microscopy measurements on Terfenol probes deposited on all the substrate types. When depositing on Pt/Si layer we observe the existence of large spherical formations, which have proven to be quantities of alloy melted during the deposition process (Fig. 4).

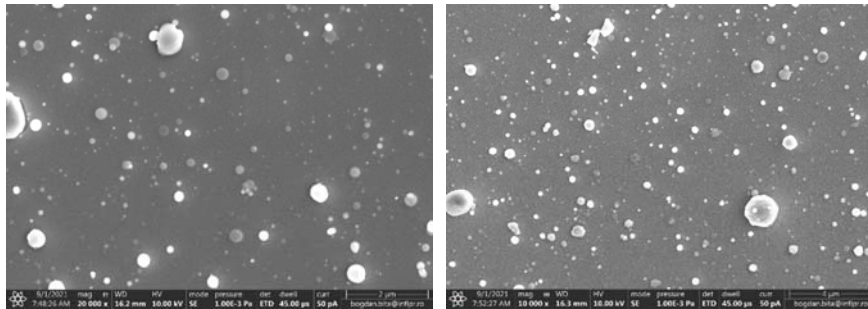


Fig. 4 – SEM pictures for Terfenol-D deposited on Pt/Si.

From Energy Dispersive X-ray analysis of the same probes we may conclude that besides the constituent elements of the metallic alloy (Tb, Dy, Fe) and Si, Pt from the used substrates, there is also a 10–15% of oxygen, which denotes that the deposition pressure of  $10^{-5}$  mbar was not low enough in order to remove all of the residual oxygen from the vacuum chamber (Fig. 5).

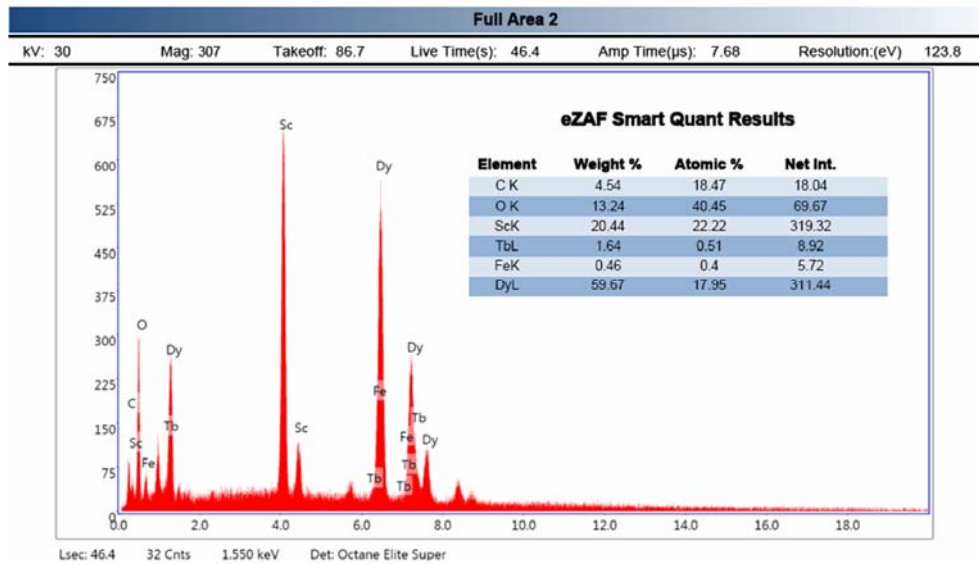


Fig. 5 – EDX for a Terfenol probe deposited on SrTiO<sub>3</sub> substrate at temperature 600°C.

This clear presence of the oxygen made us reach the conclusion that at least a part of the metallic alloy is oxidized.

Terfenol-D is a magnetostrictive alloy which shows a phase transition dependent on its concentration – Fig. 6. We have analyzed the resistance variation with temperature and magnetic field for a series of thin films deposited on both Si and Pt/Si substrates, with the help of a LakeShore HMS 8400 cryostat.

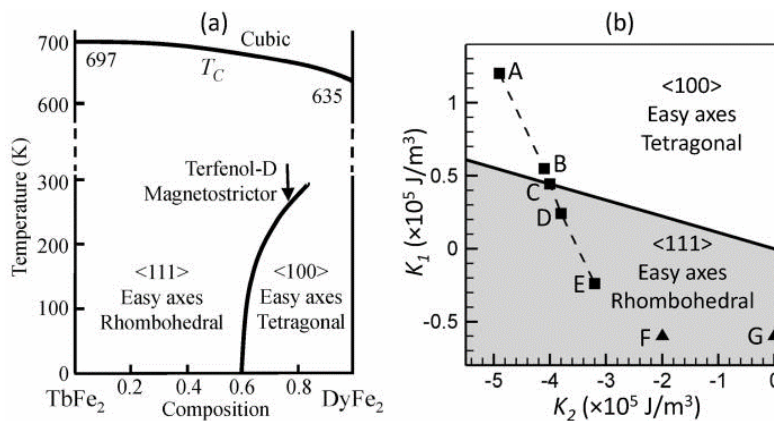


Fig. 6 – Phase transition diagram for Terfenol-D [19].

In the resistance of 0.7 Terfenol films deposited on Pt/Si substrates, as a function of temperature, we observe the large fluctuation at room temperature, but

a linear dependence as the temperature of the substrate is increased at 300°C, 500°C and 600°C (Figs. 7, 8). At around 100 K we can guess a phase transition in which Terfenol 0.7 changes its concentration to 0.6 and passes from a tetragonal structure to a rhombohedral one (see Fig. 6).

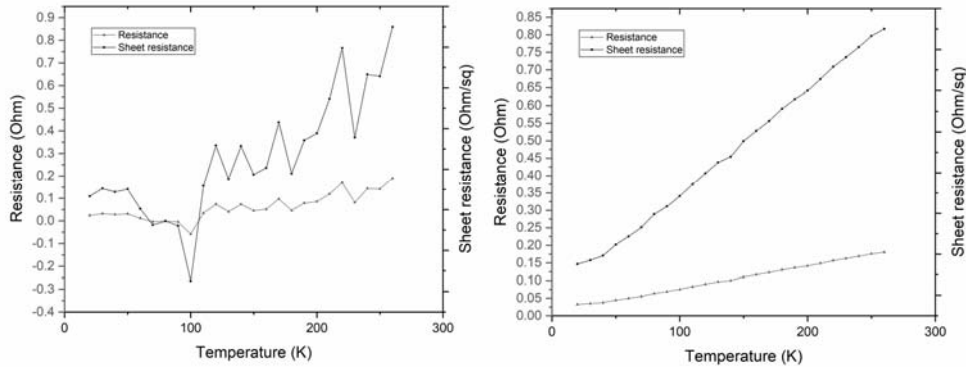


Fig. 7 – Probe 887 deposition temp RT (left), probe 888 deposition temp 300°C (right).

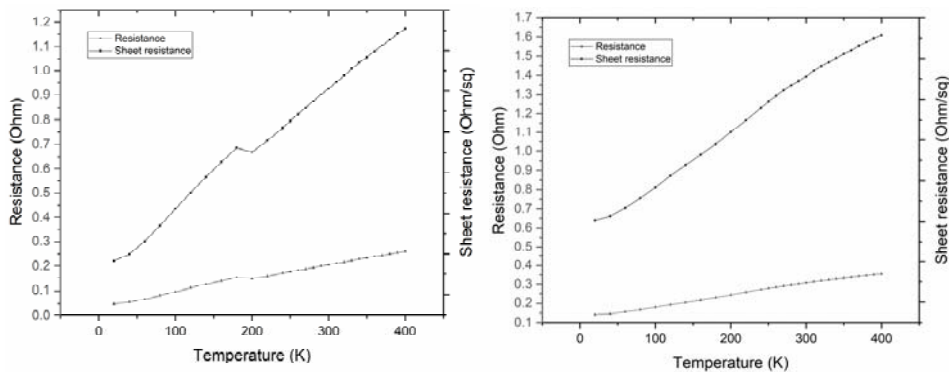


Fig. 8 – Probe 882 deposition temp 500°C (left), probe 889 deposition temp 600°C (right).

For 0.6 Terfenol the plot of resistivity at 300°C turns out to be noisier and similarly, we can observe a phase transition at about 180 K (Fig. 9), while for 500°C and 600°C substrate temperature, the dependence becomes again linear, denoting no phase transitions (Fig. 10).

In order to examine the resistivity dependence with the magnetic field we have chosen two probes, numbered 889 and 877. The measurements were done in the configuration presented in Fig. 11, at a temperature of 250 K. Looking at the dependence with the field for the Terfenol probes deposited on Pt/Si at 600°C and 500°C, we spot that for increasing temperatures the signal's noise amplifies and we have a small variation of the measured resistance. In the case of a temperature drop there is however, an increasing variation from a field of intensity of  $-1$  Tesla to

+1 Tesla. This type of behavior is in a somewhat measure similar to the Terfenol's characteristics, knowing that it is a magnetostrictive material. Even so, the difference is still very small.

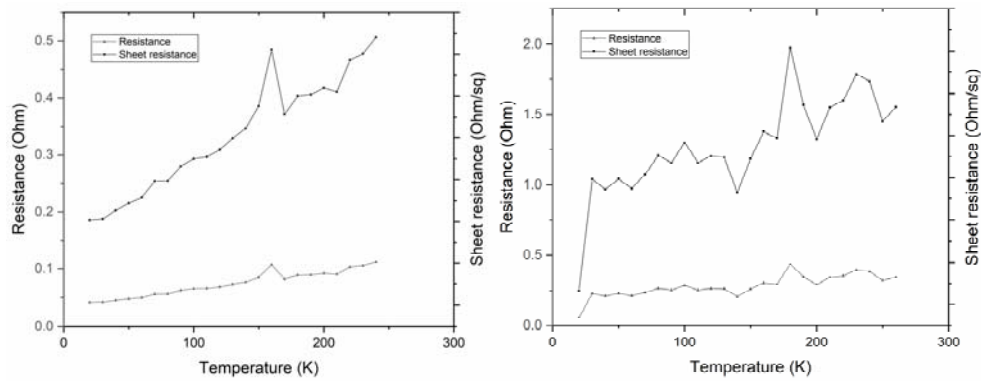


Fig. 9 – Probe 879 deposition temp RT (left), probe 878 deposition temp 300°C (right).

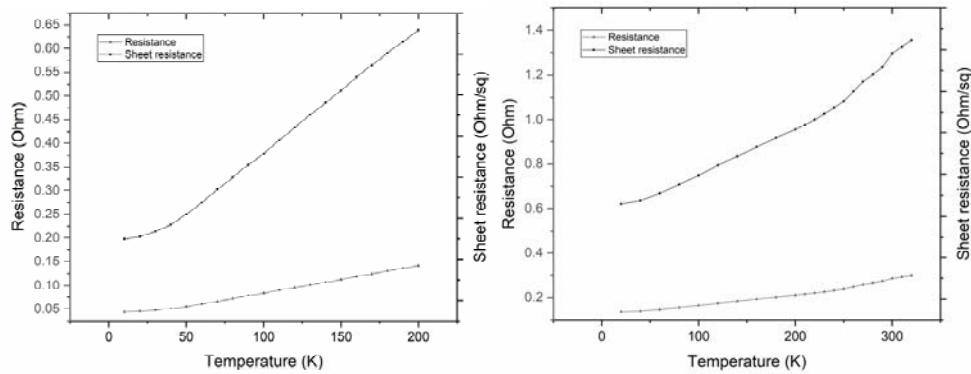


Fig. 10 – Probe 880 deposition temp 500°C (left), probe 877 deposition temp 600°C (right).

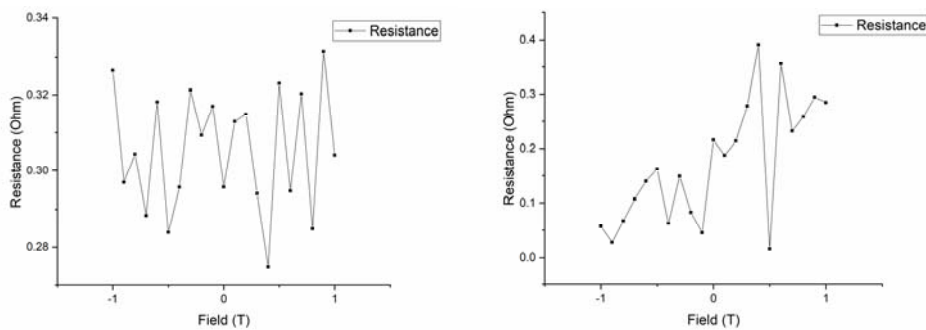


Fig. 11 – Measured resistance for Terfenol on Pt/Si probes as a function of the magnetic field's variation.

The optical analysis of the films was performed using spectroscopic ellipsometry which is a very sensitive experimental technique used for the study of thin film layer thickness and optical properties [20]. It is also an indirect measurement technique which requires us to fit the experimentally obtained data by the means of a model.

Typical ellipsometry measurements analysis consist in the comparison of the experimental data with a generated model. The first step is to measure a sample with our VASE spectrometer and determine the  $\psi$  and  $\Delta$  parameters.  $\Delta$  is the phase difference between s and p reflected light and  $\tan(\psi)$  represents the magnitude of the Fresnel coefficients ratio,  $R_p/R_s$ , using the p- and s-components of the elliptical polarized light. Then, a model is constructed using proper dispersion equations. This is done by entering all known sample properties, followed by providing our best possible guess for the unknown substrate properties [21]. Next, the software will adjust the sample properties in order to provide the best match between the computed model and the experimental plots. An indication of the “goodness of a fit” is given by the MSE (Mean-Squared-Error); the lower it is, the better the fit becomes [21].

The obtained parameters by spectroscopic ellipsometry, in which we are mostly interested in, are the thicknesses and the optical constants, given by the complex refractive index ( $N = n + ik$ ), where  $n$  is the real part (the refractive index) and  $k$  the imaginary one – extinction coefficient (at  $k = 0$  the material is said to be transparent).  $N$  is equal to square root of the dielectric function. Moreover, in the ellipsometric analysis we obtained the roughness of our probes.

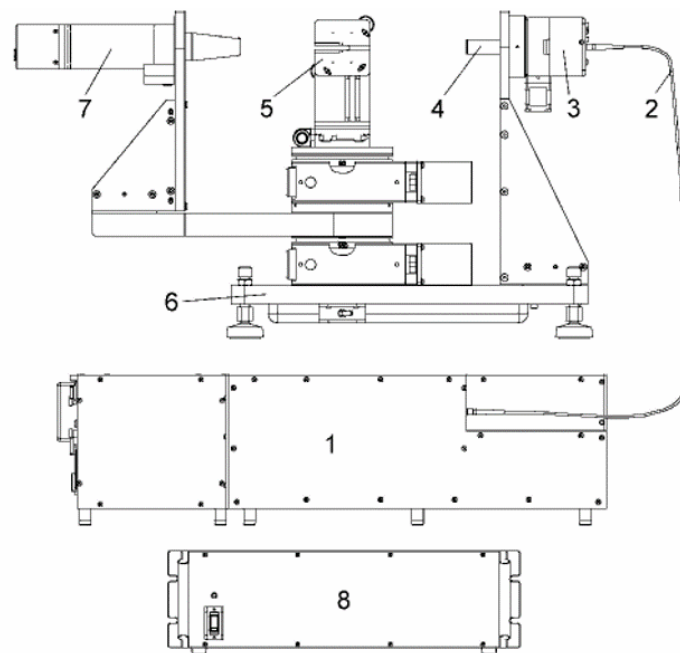


Fig. 12 – Variable Angle Spectroscopic Ellipsometer (VASE).

The experimental device is a Variable Angle Spectroscopic Ellipsometer (whose layout is given in Fig. 12) and has the following components [20]:

1. monochromator
2. fiber optic cable
3. input unit with polarizer
4. alignment detector
5. sample stage
6. goniometer base for automated angle control
7. detector unit with rotating analyzer and solid state detectors
8. motor control box.

In the optical analysis we have constructed two models depending on the used substrate. For Si substrates the first two layers are given by Si of 1 mm thickness followed by SiO<sub>2</sub> (silica) of 5 nm, as silicon oxidizes almost instantly upon atmosphere exposure. For platinum probes the SiO<sub>2</sub> layer is replaced by a Pt one which has an implicit thickness of 150 nm. Afterwards follows a genosc layer, more precisely a Lorentz oscillator layer which fits our probes after the amplitude, energy in eV and broadening of the oscillations, an EMA (effective medium approximation layer) used for the fitting of the iron oxides formation at the surface of the probes and a roughness layer.

5	srough	42.304 nm
4	SimpleGradedIndex (EMA)	250.567 nm
3	EMA (genosc)/1.19% fe_g	0.000 nm
2	genosc	0.000 nm
1	sio2_jaw	5.000 nm
0	si_jaw	1 mm

5	srough	38.081 nm
4	SimpleGradedIndex (EMA)	51.362 nm
3	EMA (genosc)/2.61% fe_g	0.000 nm
2	genosc	0.000 nm
1	pt	150.000 nm
0	si_jaw	1 mm

Fig. 13 – 873 (top) and 889 (bottom) optical models constructed through WVASE software.

In order to analyse the dispersion equation and fit the optical constants the choice was made to work with a Lorentz model. Lorentz model arises from the assumption that electrons behave as oscillating particles, due to the action of an electric field  $E$ , bound through strings to the nucleus [22]. Its specific formula comes from the solution of the electron in the imagined conditions

$$\tilde{\varepsilon}(\omega) = 1 + \frac{\omega_p^2}{\omega_t^2 - \omega^2 + i\Gamma_0\omega}, \quad (1)$$

with  $\omega_t$  resonant frequency of the oscillator expressed in eV,  $\Gamma_0$  the broadening of an oscillator and  $\omega_p$  the plasma frequency [23]. In the WVASE software all oscillator models can be used by adding the Genosc (General Oscillator) Layer, whose function is to make possible the combination of different models to enhance the obtaining of the dielectric function [10], written as:

$$\varepsilon = \varepsilon_1 + i\varepsilon_2. \quad (2)$$

The dielectric function in the selected model is fitted after the equation:

$$\varepsilon_{n_{Lorentz}} = \frac{A_n Br_n E_n}{E_n^2 - E^2 - iBr_n E}, \quad (3)$$

where  $n$  represents the number of oscillations, and  $A_n$  the amplitude (dimensionless),  $E_n$  (eV) the energy and  $Br_n$  the broadening of a peak (eV) are the fit parameters [20].

Upon the thin films, iron oxides were formed, thus the EMA layer fits the percentage of Fe concentration at the surface. The presence of the iron oxides will modify the analysed refractive index  $n$  from values specific to metals into refractive indices values closer to oxides.

To increase the efficiency of the model we use the function of simple graded index of the effective medium approximation layer. This imposes the slicing of the material, creating a series of pieces that will be described by slightly different optical constants. Generally, odd number of sublayers are preferred and we have worked by splitting the layer in 3 and 5 parts. The best number of sublayers to be used can be approximated by looking at the changes in the MSE (mean squared error) values, opting for the lowest one.

Finally, a srough.mat layer is added which represents nothing else than a different special type of EMA layer, with the utility of assessing the surface roughness of the material. It works by forming a 50% EMA layer between the top layer in the model and the ambient material [20].

Fitting the models after the oscillator parameters  $A_n$ ,  $E_n$ ,  $Br_n$ , we obtained a detailed analysis regarding the thickness of the films, the roughness values and the concentration of Fe on their surface. All these parameters, together with the MSE are presented in Table 1 for all probes. Take notice that probes from 873 until 880 have a 0.6 Dy concentration, while 881 and the following ones, until 889, have a 0.7 concentration (Table 1).

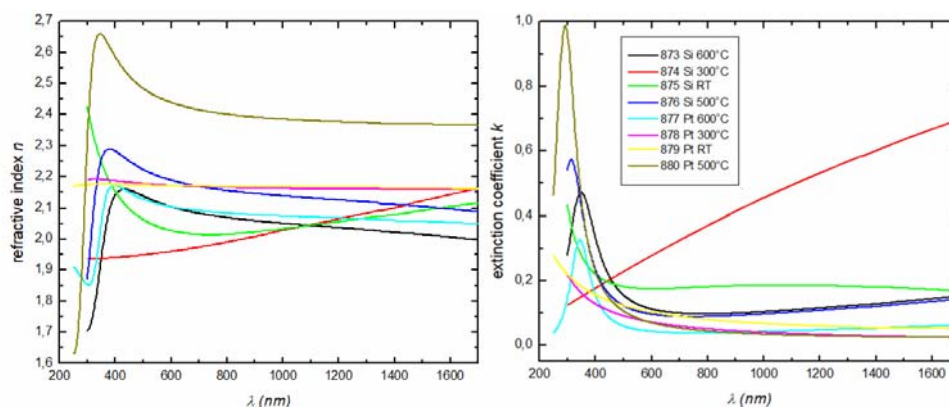
Table 1

Characteristics of probes

No. Probe	MSE	Amp	$E_n$	$Br$	Thicknes $s$	Roughnes $s$	Fe [%]
873	22.46	1.7615	3.54	1.3386	250.567	42.304	1.19
874	19.57	1.2537	1.4941	10	204.357	12.683	1.24
875	7.591	9.0826	5.6032	1.5119	212.417	11.294	2.02
876	46.59	2.278	3.9174	1.3356	193.810	32.717	1.19
877	20.55	1.2876	3.5924	0.92724	159.268	24.889	0.622
878	18.52	1.6862	6.4763	4.5304	168.873	1.175	0.0225
879	24.52	2.2615	10.492	10	151.696	13.595	0.174
880	18.9	4.4368	4.1553	1.2247	126.508	21.972	0.0968
881	16.01	2.1349	3.6622	0.97221	197.360	43.914	2.48
882	21.8	1.2318	3.48	0.86691	190.021	29.508	0.425
883	12.61	3.9119	9.5316	10	122.698	11.229	0.263
884	1.277	3.4532	6.1654	4.4312	152.431	4.642	2.79
885	12.44	1.1522	3.1986	1.1113	175.472	15.744	3.41
887	4.927	1.6212	5.455	5.9365	94.227	11.740	2.22
888	2.547	3.0672	5.3145	5.292	85.105	10.227	3.63
889	4.81	1.4311	4.8019	5.628	51.362	38.081	2.61

To comment about the thickness of the material, we can observe that the values are bigger for 0.6 probes and decreasing for 0.7. On the other hand, the iron concentration is somewhat larger for 0.7 films compared to 0.6. The roughness of the films is not very large, its biggest value reaching 43.914 nm (Figs. 14 and 15).

In the following we present the dispersion of optical constants for 0.6 Terfenol films. Normal dispersion is characterized by increasing of the refractive index with the decreasing of wavelength, or put in other words – decreasing of  $n$  with increasing of  $\lambda$ .

Fig. 14 – Dispersion of optical constants for 0.6 Terfenol (left –  $n$  vs  $\lambda$ , right –  $k$  vs  $\lambda$ ).

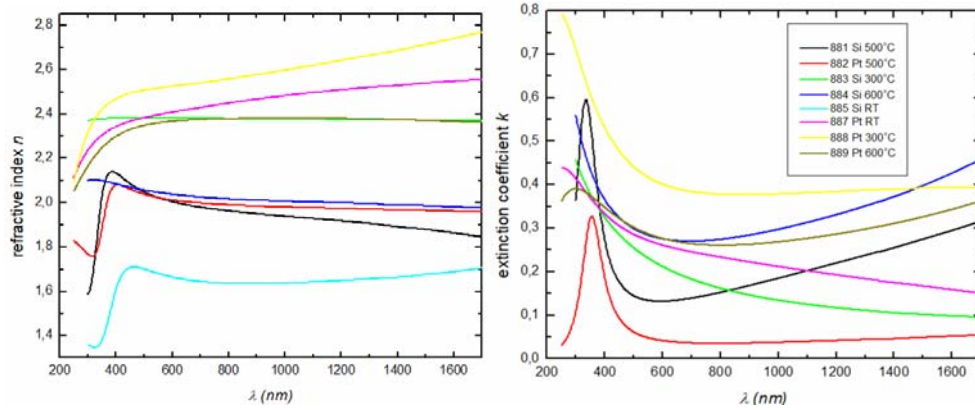


Fig. 15 – Dispersion of optical constants for 0.7 Terfenol (left –  $n$  vs  $\lambda$ , right –  $k$  vs  $\lambda$ ).

The only metallic behavior is shown by the 874 probe which was deposited on Si at the substrate temperature of 300°C, an anomalous dispersion characterized by the increase of both  $n$  and  $k$  with the increase of  $\lambda$ . All other probes present a normal dispersion and oxides conduct.

For 0.7 Dy concentrations the registered refractive indices for the RT and 300°C probes are obviously increasing in value with the decrease of the wavelength, denoting an anomalous dispersion. Also, the extinction coefficient values increase, (especially for the probes having substrate temperatures of 300°C and 600°C), getting further from the null value specific to transparent materials.

Thus, for 0.7 Terfenol the metallic character was obtained for all samples except the sample grown at 500°C temperature. Probe 881 deposited on Si is the only one with a clear decrease of  $n$  as a function of wavelength.

We could argue that generally, better results were obtained for 0.7 Dy concentration thin films.

#### 4. DISCUSSION

Optical measurements have been conducted with the help of a Woollam Vase spectroscopic ellipsometer, in the range 250–1700 nm, by a pace of 2 nm. The optical model we have used in order to fit the experimental data was constructed by a sequence of multiple layers, more precisely: the substrate (Si or Pt), the Terfenol layer and a rough layer. In the fitting process, we have tried to find a dispersion function for Terfenol which would have provided a small value of MSE (mean squared value).

The smallest values of MSE were obtained using Lorentz oscillators.

We have generated dispersion curves for the studied probes, and we have observed that the dependences of the optical constants with the wavelength

revealed a behavior typical to oxides rather than metallic layers. In some cases, there have been obtained thin films where the metallic behavior is predominant.

The presence of oxygen within the Terfenol films indicates that the deposition parameters are not optimal for the obtaining of pure metallic layers. Errors may occur due to the working pressure, temperature, nature of the substrate, etc.

Oxidation may also occur due to the exposure to atmosphere – in the time the probes arrive at the ellipsometer to be analyzed, they have already formed oxides.

## 5. CONCLUSIONS

An important conclusion is that we have not obtained pure metallic Terfenol, in all the paper we deal with an alloy which displays oxides caused by erroneous deposition conditions. The closest dispersion to that of metals were obtained for the sample deposited on Silicon at 300°C for 0.6 Terfenol and all 0.7 probes with the exception of the 500°C substrate temperature probe. One solution to the oxidation problem is decreasing the deposition pressure from  $10^{-5}$  to values of  $10^{-7}$ – $10^{-8}$  mbar, or coating the films with a protective metallic layer (gold or chromium).

*Acknowledgements.* The contents of this paper heavily rely on the first's author (Ruxanda Mireanu) bachelor thesis, entitled *Optical properties of oxidized Terfenol-D thin film obtained by pulsed laser deposition* and presented before the academic committee of the Faculty of Physics, University of Bucharest on 28 June 2022. Moreover, the experimental results were also displayed during the Annual Scientific Conference 2022 Meeting, held at the University of Bucharest, Faculty of Physics at the Solid State Physics and Materials Science, Optics, Spectroscopy, Plasma and Lasers section.

The authors would like to acknowledge PhD. Stdt. Ioan Mihail Ghitu from INFLPR for carrying out the electrical measurements, PhD. Stdt Enea Nicoleta from INFLPR for the PLD deposition of terfenol thin films and Dr. Brajnicov Simona from INFLPR for AFM characterization.

This work was supported by a grant of the Romanian Ministry of Education and Research, CNCS-UEFISCDI, project number PN-III-P4-ID-PCE-2020-2921, within PNCDI III and the work was performed using C400 PHOTOPLASMAT facilities acquired with POC153/2016 IN2-FOTOPLASMAT project.

## REFERENCES

1. Daniel Thomas O'Brien, *Laser ablation of a Terfenol-D microparticle aerosol and subsequent supersonic nanoparticle impaction for magnetostrictive thick films*, PhD Thesis, The University Texas, Austin, 2006.
2. R. Grössinger, R. Sato Turtelli and N. Mehmood, *Materials with high magnetostriction*, IOP Conference Series: Materials Science and Engineering **60**, 012002 (2014).
3. Göran Engdahl and Isaak D Mayergoyz, *Handbook of giant magnetostrictive materials*, Elsevier **386**, 2000.
4. Ricardo M. Silva, G. Chesini, C. J. Gouveia, A. B. Lobo Ribeiro, O. Frazão, C. M. B. Cordeiro and P. A. S. Jorge, *Magnetic field sensor with Terfenol-D thin-film coated FBG*, 22<sup>nd</sup> (OFS2012) International Conference on Optical Fiber Sensors **8421**, 580–583 (2012).

5. Jamel Alexander and Oliver Myers, *Microstructure Properties and Strengthening Mechanisms of the AS4-3501-6 Polymeric Resin With Embedded Terfenol-D Particles*, Smart Materials, Adaptive Structures and Intelligent Systems **46148**, V001T05A014, American Society of Mechanical Engineers (2014).
6. Xianfeng Liangetal, *A Review of Thin-Film Magnetoelastic Materials for Magnetolectric Applications*, Sensors **20.5** (2020).
7. ANR project SoftQC, *Superlattices of nanoparticles, Crystallography*.
8. LLC. TdVib, *Terfenol-D Physical Properties*.
9. Lei Chenetal, *The Study of Magneto impedance Effect for Magnetolectric Laminate Composites with Different Magnetostrictive Layers*, Materials **14.21** (2021).
10. A.G. Olabi and A. Grunwald, *Design and application of magnetostrictive materials*, Materials Design **29**, 469–483 (2008).
11. Goodfriend Mel *et al.*, *Application of a Magnetostrictive Alloy, Terfenol-D to Direct Control of Hydraulic Valves*, SAE Transactions **99**, 364–69 (1990).
12. Yanfei Wei, Xin Yang, Yukai Chen, Zhihe Zhang and Haobin Zheng, *Modeling of High-Power Tonpilz Terfenol-D Transducer Using Complex Material Parameters*, Sensors **22**, 3781 (2022).
13. Marcelo Dapino, *Magnetostrictive Materials*, Encyclopedia of Smart Materials, 2002.
14. Xiao Yan Lu, Hui Li, *Magnetic properties of Terfenol-D film on a compliant substrate*, Journal of Magnetism and Magnetic Materials **322**, 2113–2116 (2010).
15. Mohanchandra K. Panduranga, Taehwan Lee, Andres Chavez,, Sergey V. Prikhodko, and Gregory P. Carman, *Polycrystalline Terfenol-D thin films grown at CMOS compatible temperature*, AIP ADVANCES **8**, 056404 (2018).
16. H. Fujiwara, *Spectroscopic Ellipsometry: Principles and Applications*, Wiley, 2007.
17. Robert Eason, *Pulsed laser deposition of thin films: applications-led growth of functional materials*, John Wiley & Sons (2007).
18. Z. Liu, *4.09 – Laser Applied Coatings*, Ed. By Bob Cottis *et al.*, 2622–2635 (2010).
19. B.L. Wangand, Y.M. Jin, *Magnetization and magnetostriction of Terfenol-D near spin reorientation boundary*, Journal of Applied Physics **111**(10), 103908 (2012).
20. Guide to Using WVASE 32, *Spectroscopic Ellipsometry Data Acquisition and Analysis Software*, J.A. Woollam Company, Incorporated, 2008.
21. James Hilfiker and Harland Tompkins, *Spectroscopic Ellipsometry: Practical Application to Thin Film Characterization*, 2016.
22. Horiba, *Lorentz Dispersion Model, Technical Note*, Spectroscopic Ellipsometry TN08.
23. J.I. Arnaudasa, C. de la Fuente, M. Ciria, L. Benito, C. Dufour, K. Dumesnilb, A. del Morala, *Magnetoelastic stresses in epitaxial (110) Terfenol-D thin films*, Journal of Magnetism and Magnetic Materials **240**, 389–391 (2002).